Plasma Chem Plasma Process (2011) 31:427–439
DOI 10.1007/s11090-011-9294-3

ORIGINAL PAPER

Influence of Helium on the Conversion of Methane and Carbon dioxide in a Dielectric Barrier Discharge

N. R. Pinhão · A. Janeco · J. B. Branco

Received: 19 January 2011 / Accepted: 27 February 2011 / Published online: 19 March 2011

Abstract We have studied the production of synthesis gas and other hydrocarbons in a dielectric barrier discharge using mixtures of helium, methane and carbon dioxide. It was found that helium has a significant influence on the discharge, decreasing the breakdown voltage and increasing the rate of conversion of CH_4 and CO_2. However it also decreases the selectivities and the range of stable operating conditions for the discharge. The main products obtained were H_2, CO, C_2H_6 and C_3H_8 but traces of other hydrocarbon, carbon deposition and the formation of condensable products were also detected. The rate of conversion and conversion abilities were obtained by fitting the conversion results to a model.

Keywords Methane conversion · Synthesis gas · Carbon dioxide · Dielectric barrier discharge

Introduction

As the main constituent of natural gas, methane is a valuable resource in the chemistry industry both as a source of hydrogen and as raw material for the production of more complex hydrocarbons. One common application is the conversion of methane to synthesis gas (H_2 + CO mixture) through steam reforming. This process, however, has the disadvantages of operating at high temperature (requiring a slow start and costly materials) [1] and of the catalyst deactivating over time by poisoning.

The use of a non-thermal plasma (NTP) for methane conversion is a promising alternative and in recent years has been the subject of many studies [1–32]. The methane conversion values obtainable by an NTP are comparable or higher than those obtained by thermal process [20].

From the different types of discharges that produce NTP, dielectric barrier discharges (DBD) have the following advantages: (a) They operate at atmospheric pressure (normally

N. R. Pinhão (✉) · A. Janeco · J. B. Branco
ITN–Nuclear and Technological Institute, Estrada Nacional N 10, 2686-953 Sacavém, Portugal
e-mail: npinhao@itn.pt

in the filamentary mode), (b) have a high electron density and energy, (c) are easy to scale up [21] and (d) with the presence of a dielectric material in the discharge chamber, the coupling between the plasma and a catalyst used to improve the selectivity for selected products is facilitated.

The results found in literature involving methane mixtures can be divided into four groups:

Pure Methane The direct CH_4 conversion in a DBD is possible, even with high conversion rates. It, however, requires extreme power to achieve important conversion rates (1.5 MJ/L for 80% conversion [20]) and only H_2, hydrocarbons (C_xH_y) and solid carbon are viable products. Solid carbon even deposits on the electrodes and changes the characteristics of the electrodes and dielectrics [8]. The energy efficiency for conversion is low. The values reported in [20] correspond to a conversion ability of 2×10^{-8} mol/J.

Methane with an Oxidant A mixture of CH_4 with an oxidant is usually preferred. The most common oxidants used being O_2 and CO_2. Good results for the partial oxidation of CH_4 in DBDs have been reported (a conversion of 54% of CH_4 and >85% of O_2 [17] in the first case or >60% conversion of CH_4 and >30% conversion for CO_2 [18], corresponding to maximum conversion abilities of 7×10^{-8} mol/J for CH_4 and 3×10^{-8} mol/J for CO_2, respectively). The most significant products from these mixtures are H_2, CO, CO_2, CH_3OH and higher hydrocarbons (C_xH_y);

Methane with a Rare Gas Results of mixtures of CH_4 with a rare gas have been reported [2–5]. All the results indicate a significant increase in conversion with the rare gas concentration[1] but no significant difference between helium, argon and neon. The product selectivities are not significantly affected. Of these references, the only one that supplies data to estimate conversion abilities is the last where a gliding arc was used. In this case a conversion ability of 2×10^{-6} mol/J in pure methane and of 4×10^{-6} mol/J in methane with 85% helium or argon were obtained.

Methane with Other Gases Other gases, including C_2H_6 [2], N_2 [3, 4, 31, 32] and H_2O [32] were mixed with CH_4. The presence of these gases increase the CH_4 conversion, although less than in mixture with rare gases. The use of N_2 however leads to the formation of hydrogen cyanide, HCN. The presence of H_2O and O_2 enhances selectivity toward CO_2 over CO [32]. The energy efficiency for conversion also increases but at lesser magnitude.

The above results suggest that mixtures of CH_4, an oxidant and a rare gas provide the best results. The presence of the rare gas seems to improve the conversion of both CH_4 and the oxidant with the latter promoting the formation of oxygenated products.

In the present work we study how the helium mole fraction affects the results obtained from mixtures of CH_4, CO_2 and He in a dielectric barrier discharge reactor, without using a catalyst. We chose CO_2 as oxidant as it is an important constituent gas in many natural gas fields and both CH_4 and CO_2 are major greenhouse gases. Their simultaneous conversion into higher value hydrocarbons or synthesis gas is, therefore, of great interest. We measured the conversion of CH_4 and CO_2, the selectivities for the main products and the abilities in mixtures with different mole fractions of helium for a $[CH_4]/[CO_2]$ ratio, $\mathcal{R}$, of approximately one. Additionally we have studied the influence of $\mathcal{R}$ on mixtures with 85% of helium.

[1] Aghamir [5] concludes that the rare gas has no effect but Fig. 5 in that paper indicates otherwise.

Experimental Set-up

DBD Reactor

The experiments were performed in a cylindrical DBD reactor (Fig. 1) having a central Stainless Steel electrode of 5 mm diameter, supported by MACOR® fittings, inside a 10 mm I.D., 1 mm thick glass tube. The external (ground) electrode is an aluminium thin foil stretched around the glass. The chamber has a porous glass on one end, at a few millimeters from the tip of the internal electrode, used to support a catalyst. However, as mentioned before, the present results were obtained without a catalyst. At the exit of the chamber a trap cooled at 0°C collects the liquid products. The sinusoidal power supply allows a maximum *rms* voltage of 10 kV. The measurements were obtained within a (4 to 6) kHz frequency range.

In this reactor we faced the problem of the formation of an arc during the experiments, which could damage the reactor. To avoid this, we performed several measurements with the outer wall of the reactor cooled.

Mixtures of $He/CH_4/CO_2$, where the helium mole fraction varied between 50 and 95%, were studied. The ratio $\mathcal{R}$ was changed from 0.2 to 4.2. The gas flows were controlled with standard mass flow controllers. The total gas flow rate was changed from (2 to 6) L/h.

Diagnostics

A main parameter characterising the discharge is the energy density in the plasma, usually measured by the specific input energy, $\mathcal{S}$, defined as

$$\mathcal{S} = \frac{\overline{P}}{q_V} \tag{1}$$

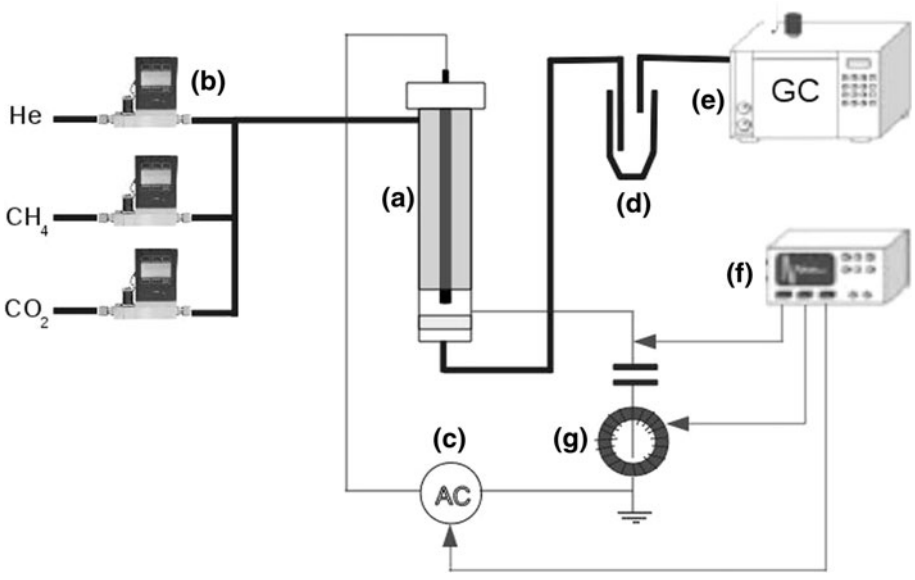

Fig. 1 Experimental set-up: (**a**) DBD chamber, (**b**) mass flow controllers, (**c**) power supply, (**d**) trap, (**e**) gas chromatographer, (**f**) oscilloscope, (**g**) Rogowsky coil

where $\overline{P}$ is the average power used on the discharge and q_V the volume flow rate of the gas mixture. However, in a discharge at constant pressure and temperature where reactions take place, the gas flow rate changes along the reactor and $\mathcal{S}$ is space dependent. On alternative $\mathcal{S}$ could be defined from a space averaged flux rate. Nonetheless, and in order to compare our results with other authors, we use the values of $\mathcal{S}$ calculated with the flow rate at the entrance of the reactor.

Using a *Tektronix*™ TDF 3052B digital oscilloscope with a sampling rate of one giga samples per second and channel, and a *Pearson*™ Rogowsky coil we acquired the signals for applied voltage, U, charge, Q, (integrating the discharge current through a capacitor), current, I, and instantaneous power, P, measured in the oscilloscope by direct multiplication of voltage and current in the oscilloscope. This allowed us to test four different methods to compute the energy consumption of the discharge system in one AC cycle (E_{cycle}) as discussed elsewhere [33]. Finally, the average power was calculated as

$$\overline{P} = E_{\text{cycle}} \cdot f \tag{2}$$

from a moving average of 10,000 points. The standard deviation of $\mathcal{S}$ is lower than 5%.

The output gas composition was analysed on-line by gas chromatography using a *Restek*™ ShinCarbon ST column ($L = 2.0$ m, $f = 1/8$ in, ID = 1 mm, 100/200 mesh) and a *Shimadzu*™ 9A GC equipped with a thermal conductivity detector (TCD) and a 6-port gas sampling valve with a 0.25 μL loop. The (1σ) uncertainty on species mole fraction is lower than one percentage point.

The quantities characterizing the reactor are usually defined as a function of the molar flow of each species. However, if we account for the change in total flow rate due to reactions, deposition or condensation and consider constant pressure and temperature conditions, we can substitute the molar flows by the value of mole fraction measured in the GC. The change in the gas flow rate can be estimated measuring the mole fraction of the inert gas in the GC, before, $[He]_0$, and during the discharge, $[He]$. From these values we can calculate an expansion (or contraction) factor for the gas, α, as

$$\alpha = \frac{[He]_0}{[He]} \tag{3}$$

The values of α in the mixtures studied ranged between 0.98 and 1.12.

Results and Discussion

We analysed two sets of mixtures: in the first set we kept the ratio $\mathcal{R}$ at a value of approximately one and changed the helium mole fraction. In the second set we kept the helium mole fraction constant at 85% and changed $\mathcal{R}$.

In all the mixtures studied the main products detected were H_2, CO, C_2H_6 and C_3H_8 although we also found traces of liquid products and solid carbon deposits.

Breakdown Voltage

The first observable effect of the composition of the gas mixture was a change in the breakdown voltage, extracted from an analysis of the Lissajous figures obtained from the applied voltage, U, and discharge current, I. The dispersion in breakdown values for a given composition obtained by this method was large but we observed a clear reduction in

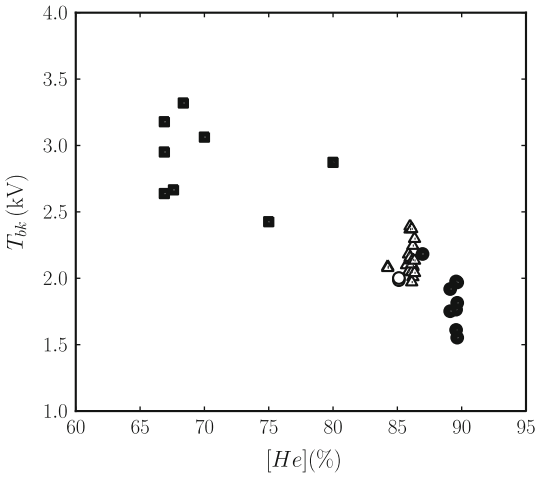

Fig. 2 Variation of the breakdown voltage with helium mole fraction in $He/CH_4/CO_2$ mixtures with different $\mathcal{R}$ ratios— *filled circle* $0.3 < \mathcal{R} < 0.9$; *filled square* $0.9 < \mathcal{R} < 1.1$; *open triangle* $1.3 < \mathcal{R} < 1.5$; *open circle* $4 < \mathcal{R}$

breakdown voltage with increasing helium mole fraction as shown in Fig. 2. On the other hand, the $\mathcal{R}$ ratio does not seem to have any influence.

The results can be explained [34, 35] by the condition for self-sustainment in inhomogeneous fields, assuming that each discharge starts as a Townsend avalanche and using the Townsend coefficient values obtained for the electron kinetics in those mixtures.

Reactants

To evaluate the efficiency of the system, we studied the values of conversion. Using the factor α defined in (3), the definition of conversion for a reactant species X is:

$$C_X(\%) = \frac{[X]_0 - \alpha[X]}{[X]_0} \times 100 \tag{4}$$

The uncertainty in C_X, in general, is comparable with the uncertainty in mole fraction. However, as some values are obtained by subtraction of values of similar magnitude, the relative uncertainties can increase significantly.

Within the range of $\mathcal{S}$ studied, the conversion of both reactants increase linearly with $\mathcal{S}$, as shown in Figs. 3 and 4. Helium mole fraction has a significant impact on the slope of these curves (Fig. 3) for both reactants. As discussed in [36] this is explained by a shift in the electron energy distribution to higher energies with helium mole fraction and, consequently, an increase in the rate coefficients for reactions between the electrons and the molecular gases. The authors have also found [35] that, except for the highest values of helium mole fraction, the collision frequencies for processes in helium are much smaller than in the other two gases indicating that helium excited states and ions have a minimal or no role in the discharge.

As a rule, the effect of $\mathcal{R}$ is to increase the conversion of a reactant when its mole fraction decreases (Fig. 4). In CO_2, however, this rule is only observed when $\mathcal{R} < 1$. Above $\mathcal{R} \approx 1$ the CO_2 conversion seem to become independent of $\mathcal{R}$ and all the values fall within the experimental uncertainty.

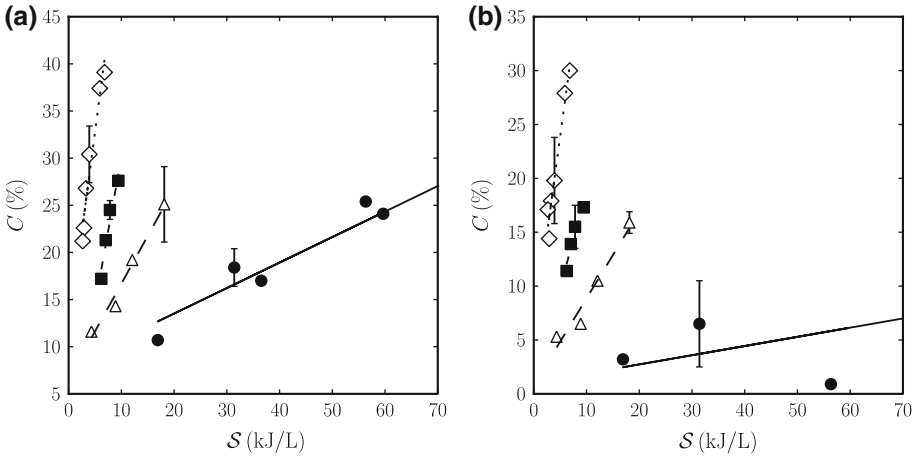

Fig. 3 Dependency of conversion for (**a**) CH_4 and (**b**) CO_2 with the specific energy in mixtures with $\mathcal{R} \approx 1$ and different values of helium mole fraction: *filled circle*, *solid line* 55%, *open triangle*, *dashed line* 75%, *filled square*, *dashed dotted line* 85%, *open diamond*, *dottedline* 95%. *Symbols* experimental values, *lines* regression curves. For each set of data only a representative error bar is indicated

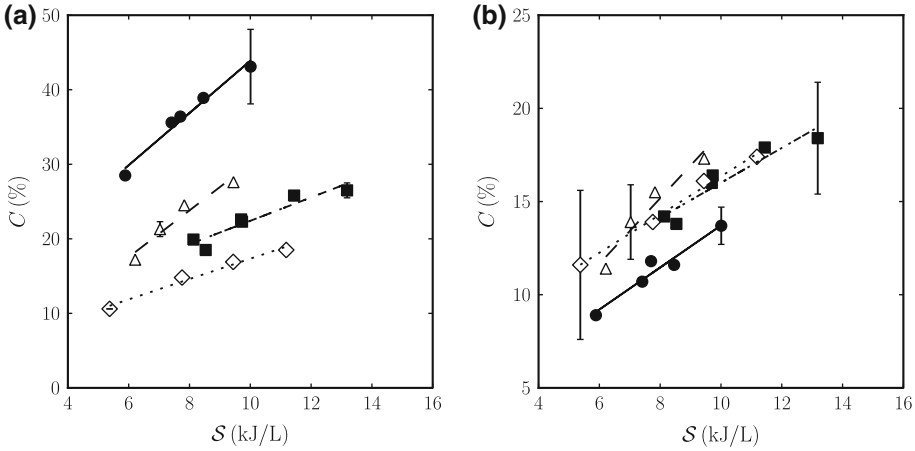

Fig. 4 Dependency of conversion for (**a**) CH_4 and (**b**) CO_2 with the specific energy in mixtures with a helium mole fraction of 85% and different values of $\mathcal{R}$: *filled circle*, *solid line* 0.2, *open triangle*, *dashed line* 0.9, *filled square*, *dashed dotted line* 1.4, *open diamond*, *dottedline* 4.2. *Symbols* experimental values, *lines* regression curves. For each set of data only a representative error bar is indicated

The linear dependency of conversion on $\mathcal{S}$ observed in these figures can be understood through a simple model. We assume that the mole fraction of reactants decreases exponentially with the energy consumption per mole, $\mathcal{S}/c$,

$$[X] = [X]_0 \exp\left(-\frac{\mathcal{S}}{c} \cdot \zeta_X\right) \alpha^{-1} \tag{5}$$

Table 1 Results obtained in He/CH_4/CO_2 mixtures for different values of helium mole fraction and [CH_4]/[CO_2] ratio, $\mathcal{R}$

[He]		ζ(μmol/J)		$C_X(0)$ (%)		*r*/*t*	*s*/*t*	[H_2]/[CO]
%	$\mathcal{R}$	CH_4	CO_2	CH_4	CO_2			
55	1.2	0.14(3)	0.04(2)	6(2)	1(4)	0	–	0.8
75	1.0	0.45(7)	0.36(6)	6(2)	1(2)	1.3–1.9	4.6–7.6	0.8
85	0.2	1.6(2)	0.50(8)	9(3)	2(1)	0.6	1.5–1.7	0.37
85	0.9	1.4(2)	0.8(1)	−1(4)	1(2)	1.2	3.2–3.4	0.88
85	1.4	0.7(1)	0.4(1)	7(3)	7(2)	1.5–1.6	3.9–4.2	1.27
85	4.2	0.61(8)	0.46(5)	4(1)	6(1)	2.6–2.7	6.4–6.6	4.19
95	0.9	1.9(3)	1.6(2)	11(3)	6(2)	1.0–1.2	2.4–4.4	0.8

For the meaning of the symbols, see the text. The numbers in parentheses are the standard uncertainties of the last digit of the result

where c is the amount concentration, ζ_X is the rate of conversion of X moles divided by energy transferred to the gas and α accounts for the change in number of molecules from reactions (as defined in (3)).

For small values of the exponent the conversion (4) becomes,

$$C_X \approx \frac{\mathcal{S}}{c} \cdot \zeta_X \times 100 \tag{6}$$

which justifies the linear dependency observed. The values of ζ_X for each mixture and reactant, obtained from a linear regression of the data on Figs. 3 and 4, are summarised in Table 1.

According to (6) the intersection of the regression line with the conversion axis should be null. However Table 1 shows that several regression lines exhibit a positive intercept value. This can be explained by an overestimation of the values of $\mathcal{S}$ when using the flux at the entrance, as discussed in section "Diagnostics". If the flux inside the reactor is higher than the flux at the entrance (and increases with conversion) the correct values of $\mathcal{S}$ are smaller than indicated in the figures. A reduction of the $\mathcal{S}$ values would increase the slope of the regression lines and decrease the value of the intercept.

Products

The production of synthesis gas and other hydrocarbons was evaluated by looking at how the input atoms are distributed across the products, as measured by the values of selectivity, defined as

$$S_{Y,z}(\%) = \frac{\alpha n_{Y,z}[Y]}{\sum_X n_{X,z}([X]_0 - \alpha[X])} \times 100 \tag{7}$$

where $S_{Y,z}$ is the selectivity for product Y regarding the z atom balance, $n_{X,z}$ is the number of atoms z in species X, and the sum is for all reactants containing z atoms. We studied the values of selectivity for CO, C_2H_6 and C_3H_8 for the balance of carbon atoms and the selectivity for H_2. Taking into account (4), (7) and the definition of $\mathcal{R}$, the selectivities for C_nH_m products for the balance of hydrogen atoms and for CO for the balance of oxygen atoms, can be deduced from the corresponding selectivities for the balance of carbon atoms as

$$S_{C_nH_m,H} = \frac{m}{4n}\left(\frac{C_{CO_2} + \mathcal{R}\cdot C_{CH_4}}{C_{CO_2}}\right) S_{C_nH_m,C} \tag{8}$$

$$S_{CO,O} = \frac{1}{2}\left(\frac{C_{CO_2} + \mathcal{R}\cdot C_{CH_4}}{C_{CO_2}}\right) S_{CO,C} \tag{9}$$

Finally we determined the selectivity for conversion of hydrogen or carbon atoms into other products, including liquid products, as

$$S_{other,z}(\%) = 100 - \sum_{Y} S_{Y,z}(\%) \tag{10}$$

where z is H or C and the sum is for hydrogen, ethane and propane for the H balance, and on carbon monoxide, ethane and propane for the C balance, respectively.

The uncertainties increase with the mole fraction of helium such that the results for 85% and 95% helium cannot be distinguished from each other. Nonetheless Figs. 5 and 6 show that the selectivities for CO, C_2H_6 and H_2 decrease when the helium mole fraction increases and, for a given mole fraction of helium, are either independent of or have a small dependency on $\mathcal{S}$. However the selectivities for C_3H_8 continue to increase with $\mathcal{S}$. Other selectivities are not shown as, according to (8) and (9), they follow the same trend as the corresponding selectivities in terms of carbon atom balance. An explanation for the decrease in selectivity with an increase in helium mole fraction is again the increase in the

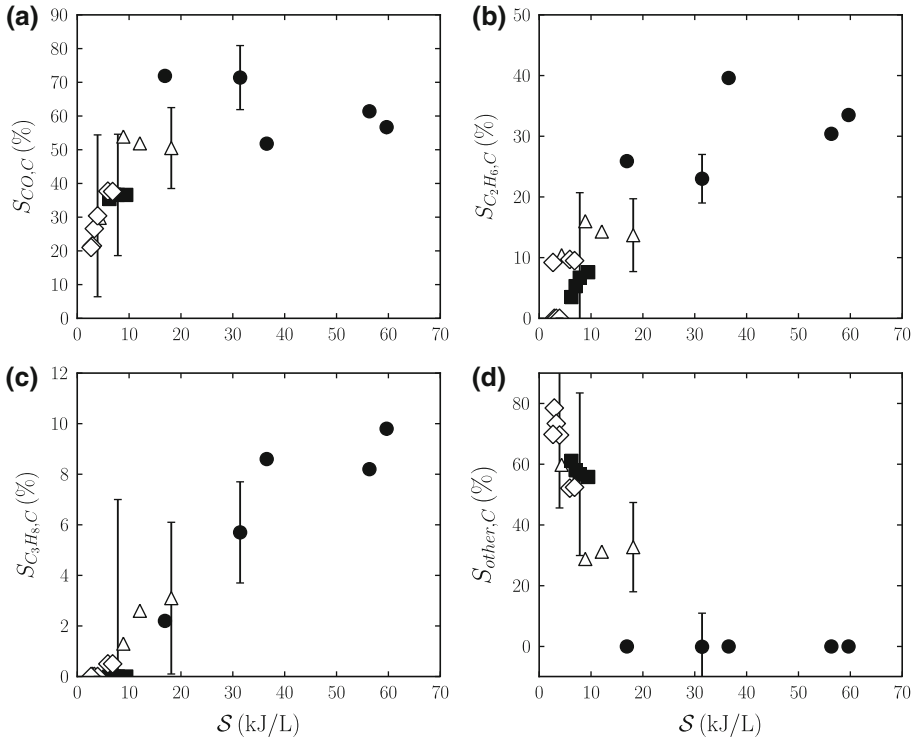

Fig. 5 Selectivity regarding the C atoms balance for (**a**) CO, (**b**) C_2H_6, (**c**) C_3H_8 and (**d**) remaining products, for mixtures with $\mathcal{R} \approx 1$ and different mole fractions of helium. *Symbols* and *error bars* as in Fig. 3

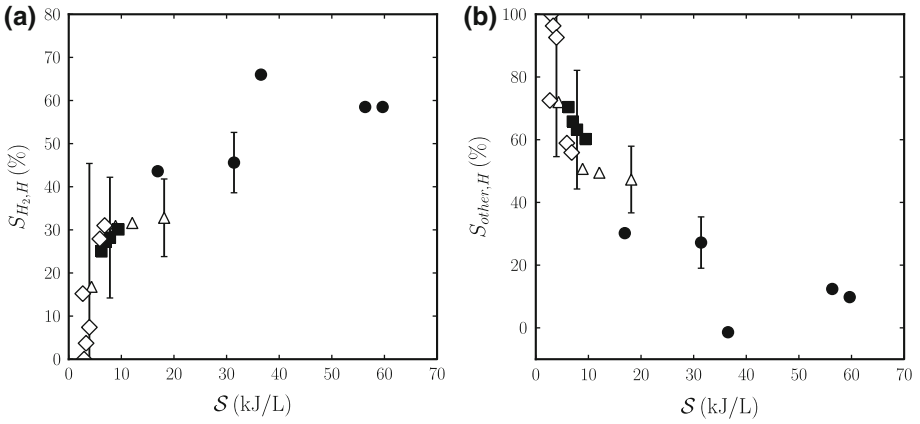

Fig. 6 Selectivity regarding the H atoms balance for (**a**) H_2, (**b**) remaining products. Mixtures, *symbols* and *error bars* as in Fig. 5

electron rate coefficients as helium increases. As the total rate of production for each product in the discharge is a balance between formation and decomposition, the increase in the electron collision rates also increases the decomposition of these products.

Figures 5d and 6b show that for the mixture with 55% helium, practically all carbon atoms are converted into the three products indicated while 20% of the hydrogen atoms are converted into products other than H_2. The same happens with part of oxygen atoms as the only gas detected containing oxygen atoms, CO, does not account for all the oxygen atoms converted in the reactor. As the mole fraction of helium increases, the fraction of carbon and hydrogen atoms converted that are not detected in the gas phase also increases. The formation of condensable products that are retained in the trap or deposited in the reactor can account for this missing fraction. In fact we observed deposition of a carbon film in the reactor and formation of drops in the trap although further identification has yet to be conducted.

Nevertheless, we can estimate the liquid products that could have been formed. Let us assume that the mixture of deposited and condensed products is represented by a chemical compound with empirical formula $C_rH_sO_t$, where r, s and t are real numbers. Using (7–10) it can be shown that

$$\frac{r}{t} = \frac{S_{\mathrm{CO,O}}}{S_{\mathrm{CO,C}}} \left(\frac{100 - \sum_Y S_{Y,C}}{100 - S_{\mathrm{CO,O}}} \right) \tag{11}$$

$$\frac{s}{t} = 2 \frac{[\mathrm{H_2}]}{[\mathrm{CO}]} \frac{S_{\mathrm{CO,O}}}{S_{\mathrm{H_2}}} \left(\frac{100 - \sum_Y S_{Y,H}}{100 - S_{\mathrm{CO,O}}} \right) \tag{12}$$

The range of r/t and s/t ratios obtained for each mixture are indicated in Table 1. These values are compatible with the formation of water (H_2O), formaldehyde (CH_2O), methanol (CH_3OH), ethanol (C_2H_5OH) and, for the mixture with $\mathcal{R} = 4.2$, isopropyl alcohol ($(CH_3)_2CHOH$) or its isomer, propanol.

Concerning the effect of $\mathcal{R}$, changing this ratio has a strong influence on the selectivity for CO regarding the C atom balance (Fig. 7a) and on the range of r/t and s/t values, but has no significant effect on H_2 selectivity (Fig. 7b).

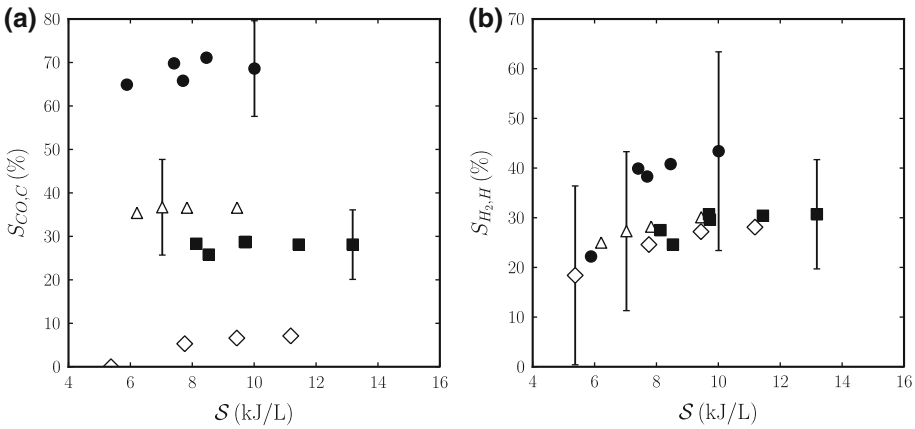

Fig. 7 Influence of ratio $\mathcal{R}$ in mixtures with 85% of helium on selectivity for (**a**) CO regarding the C atoms balance and, (**b**) H_2. *Symbols* and *error bars* as in Fig. 4

The $[H_2]/[CO]$ balance is practically independent of the mole fraction of helium but depends on $\mathcal{R}$ as indicated in Table 1.

Energy Efficiency

The energy efficiency for conversion of species X or conversion ability [3], is defined as

$$\eta_X = \frac{[X]_0 - \alpha[X]}{\mathcal{S}/c} \tag{13}$$

Similarly, the energy efficiency for production of species Y or production ability [3], is defined as

$$\eta_Y = \frac{\alpha[Y]}{\mathcal{S}/c} \tag{14}$$

Taking into account (4) and (6), the relationship between the conversion ability, η_X and the rate of conversion, ζ_X, is

$$\eta_X = \zeta_X [X]_0 \tag{15}$$

Figure 8 shows that the conversion abilities for CH_4 and CO_2, in mixtures with $\mathcal{R} \approx 1$, increase with helium mole fraction until a maximum of around 80%, decreasing thereafter.

These values correspond to a minimum energy consumption of 5.7 MJ/mol for the mixture with 85% helium. In this case, the energy consumption for the dissociation of CH_4 and CO_2 were 9 MJ/mol and 14 MJ/mol for CH_4 and CO_2, respectively. These values are comparable to those obtained in DBD discharges driven by AC power supplies in pure CH_4 [20] (estimated in 40 MJ/mol) and in CH_4/CO_2 mixtures [18] (minimum values of 8.6 MJ/mol for the mixture, with 15 MJ/mol for CH_4 and 20 MJ/mol for CO_2).

Although the admixture of helium reduces the energy consumption per mole, these values are still high for commercial application. Moreover, the separation of helium from the products adds another step to the process. The combination with a catalyst and/or a pulsed power supply is necessary to improve the efficiency of the process.

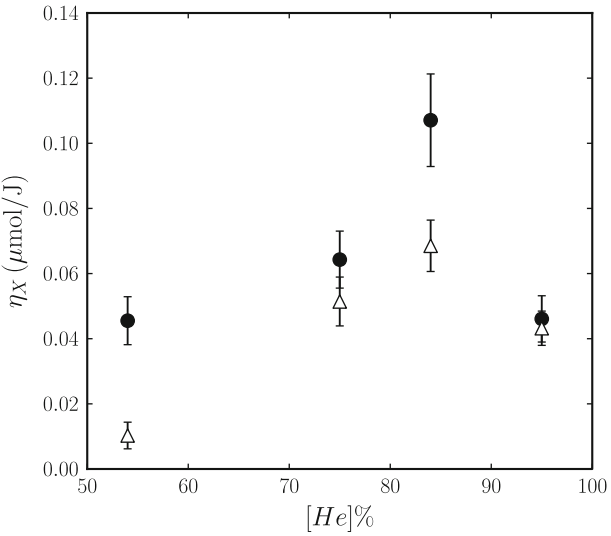

Fig. 8 Dependency of conversion ability on helium mole fraction in mixtures with $\mathcal{R} \approx 1$. *filled circle* CH_4, *opentriangle* CO_2

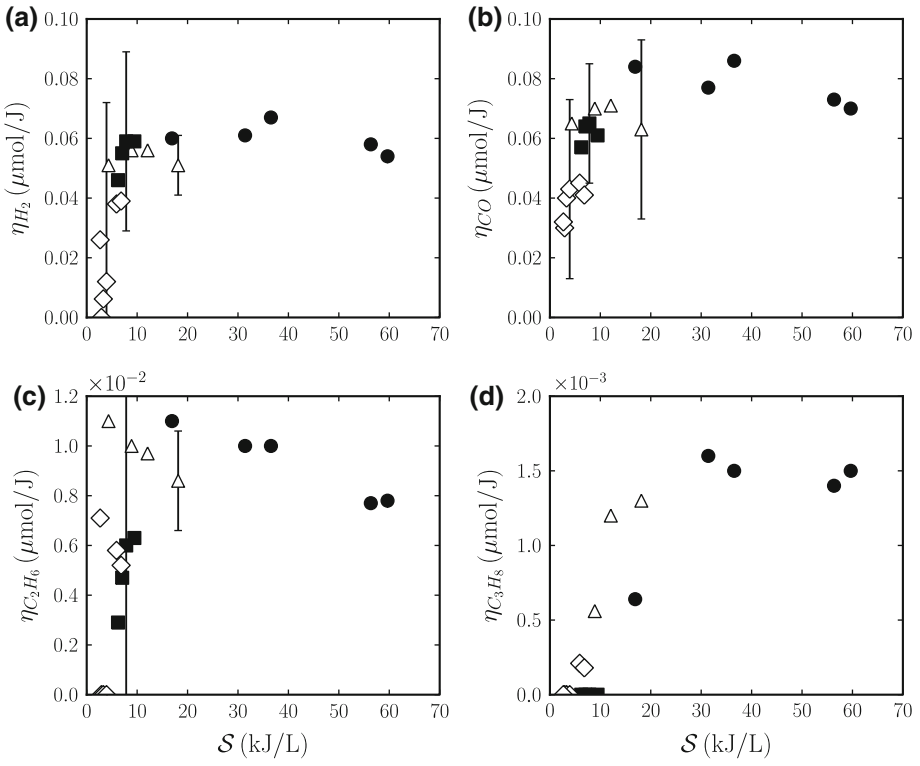

Fig. 9 Dependency of production ability on helium mole fraction in mixtures with $\mathcal{R} \approx 1$: (**a**) H_2, (**b**) CO, (**c**) C_2H_6 and (**d**) C_3H_8. *Symbols* and *error bars* as in Fig. 3

For all the products studied (H_2, CO, C_2H_6 and C_3H_8), the production abilities (Fig. 9) seem to decrease with helium mole fraction. Unfortunately the uncertainties in the results for mixtures with the highest helium mole fractions are large. For low values of $\mathcal{S}$ and until approximately 10 kJ/L, or 30 kJ/L for C_3H_8, the production abilities increase with $\mathcal{S}$ and become constant or slightly decrease at higher $\mathcal{S}$ values.

Conclusions

In this work we reported experimental results for the oxidation of CH_4 in the presence of CO_2 and helium in a dielectric barrier discharge. Although the main focus of the study was on the influence of helium, we have also studied the effect of the $[CH_4]/[CO_2]$ ratio.

The main products obtained were H_2, CO, C_2H_6 and C_3H_8 but several other hydrocarbons were also detected. Deposition of carbon was observed as well as the formation of condensable products.

We observed that the presence of helium has a significant influence on the discharge, namely on the breakdown voltage, the rate of conversion of CH_4 and CO_2 and, at a smaller scale, on selectivities. A high mole fraction of helium is beneficial as it decreases the breakdown voltage and increases the rate of conversion of reactants. The highest energy efficiency in conversion is obtained at a helium mole fraction of around 80%. A high helium mole fraction, however, has also detrimental effects as the range of stable conditions for the discharge decreases as well as the values of selectivity.

The conversion of CH_4, the CO selectivity regarding the C atom balance, the $[H_2]/[CO]$ balance and the mixture of liquid products can be improved by changing $\mathcal{R}$. The production of Syngas or any specific product can be optimized by careful selection of helium mole fraction and $\mathcal{R}$.

A model of the electron and chemical kinetics of these mixtures can be a valuable tool to explain the results observed and help to optimize the conversion of CH_4 and CO_2.

Acknowledgments We acknowledge the financial support by FCT under the contract number PTDC/EQU-EQU/65126/2006.

References

1. Nair SA, Nozaki T, Okazaki K (2007) Chem Eng J 132:85–95
2. Thanyachotpaiboon K, Chavadej S, Caldwell TA, Lobban LL, Mallinson RG (1998) AIChE J 44:2252–2257
3. Okumoto M, Kim HH, Takashima K, Katsura S, Mizuno A (2001) IEEE Trans Ind Appl 37:1618–1624
4. Indarto A, Choi J-W, Lee H, Song HK (2006) Energy 31:2986–2995
5. Aghamir FM, Matin NS, Jalili AH, Esfarayeni MH, Khodagholi MA, Ahmadi R (2004) Plasma Sources Sci Technol 13:707
6. Malik M, Jiang X (1999) Plasma Chem Plasma Process 19:505–512
7. Larkin DW, Lobban LL, Mallinson RG (2001) Catal Today 71:199–201
8. Liu C-J, Xue B, Eliasson B, He F, Li Y, Xu G-H (2001) Plasma Chem Plasma Process 21:301–310
9. Kraus M, Egli W, Haffner K, Eliasson B, Kogelschatz U, Wokaun A (2002) Phys Chem Chem Phys 4:668–675
10. Yang Y (2003) Plasma Chem Plasma Process 23:327–346
11. Zhang Y-P, Li Y, Wang Y, Liu C-J, Eliasson B (2003) Fuel Process Technol 83:101–109
12. Zheng G, Jiang J, Wu Y, Zhang R, Hou H (2003) Plasma Chem Plasma Process 23:59–68
13. Kado S, Sekine Y, Nozaki T, Okazaki K (2004) Catal Today 89:47–55
14. Khassin AA, Pietruszka BL, Heintze M, Parmon VN (2004) React Kinet Catal Lett 82:111–119

15. Li X-S, Zhu A-M, Wang K-J, Xu Y, Song Z-M (2004) Catal Today 98:617–624
16. Pietruszka B, Anklam K, Heintze M (2004) Appl Catal 261:19–24
17. Pietruszka B, Heintze M (2004) Catal Today 90:151–158
18. Song HK, Lee H, Choi J-W, Na BK (2004) Plasma Chem Plasma Process 24:57–72
19. Indarto A, Choi J-W, Lee H, Song HK (2005) J Nat Gas Chem 14:13–21
20. Indarto A, Choi J-W, Lee H, Song HK (2006) J Nat Gas Chem 15:87–92
21. Istadi I, Amin NAS (2006) Fuel 85:577–592
22. Istadi I, Amin NAS (2007) Chem Eng Sci 62:6568–6581
23. Kim S-S, Lee H, Choi J-W, Na B-K, Song HK (2007) Catal Commun 8:1438–1442
24. Kim S-S, Kwon B, Kim J (2007) Catal Commun 8:2204–2207
25. Naidis GV (2007) J Phys 40:4525–4531
26. Baowei W, Kuanhui Y, Genhui X (2008) Plasma Sci Tech 10:575
27. Indarto A (2008) J Chin Inst Chem Eng 39:23–28
28. Indarto A, Coowanitwong N, Choi J-W, Lee H, Song HK (2008) Fuel Process Technol 89:214–219
29. Indarto A, Yang DR, Palgunadi J, Choi J-W, Lee H, Song HK (2008) Chem Eng Process 47:780–786
30. Rueangjitt N, Sreethawong T, Chavadej S (2008) Plasma Chem Plasma Process 28:49–67
31. Jasinski M, Dors M, Nowakowska H, Mizeraczyk J (2008) Chem Listy 102:s1332–s1337
32. Mfopara A, Kirkpatrick MJ, Odic E (2009) Plasma Chem Plasma Process 29:91–102
33. Janeco A, Pinhão NR, Branco JB, Ferreira AC (2009) ISPC19-Proceedings P2.2.64:773
34. Pinhão NR, Janeco A, Branco JB, Ferreira AC (2009) ISPC19-Proceedings O16.02:669
35. Pinhão NR, Janeco A, Branco JB (2010) HAKONE XII—book of contributed papers, vol 2, pp 412–416
36. Pinhão NR, Vranic M (2010) XX ESCAMPIG—conference proceedings P1.30